Available online at www.sciencedirect.com

SCIENCE DIRECT®

Journal of Catalysis 217 (2003) 100–106

JOURNAL OF CATALYSIS

www.elsevier.com/locate/jcat

On the hydrothermal stability of CuAPSO-34 microporous catalysts for N_2O decomposition: a comparison with CuZSM-5

B.I. Palella,[a] M. Cadoni,[b] A. Frache,[b] H.O. Pastore,[c] R. Pirone,[a] G. Russo,[d]
S. Coluccia,[e] and L. Marchese [b,*]

[a] *Istituto di Ricerche sulla Combustione IRC-CNR, Piazzale V. Tecchio 80, 80125 Napoli, Italy*
[b] *Dipartimento di Scienze e Tecnologie Avanzate, Università del Piemonte Orientale "A. Avogadro," Corso Borsalino 54, 15100 Alessandria, Italy*
[c] *Instituto de Química, Universidade Estadual de Campinas, CP 6154, CEP 13083-970, Campinas, SP, Brazil*
[d] *Dipartimento di Ingegneria Chimica, Università degli Studi di Napoli Federico II, Piazzale V. Tecchio 80, 80125 Napoli, Italy*
[e] *Dipartimento di Chimica IFM, Università di Torino, Via P. Giuria 7, 10125 Torino, Italy*

Received 3 September 2002; revised 9 January 2003; accepted 16 January 2003

Abstract

The hydrothermal stability of CuAPSO-34 microporous silicoaluminophosphates with chabasite structures has been investigated and compared to that of a copper-exchanged ZSM-5 zeolite by a combined XRD, FTIR, and catalytic study. CuAPSO-34 showed a higher hydrothermal structural stability (steaming 80 h at 600 °C), as found by XRD. Spectroscopic FTIR investigation of adsorbed CO revealed that upon this steaming procedure the concentration of monovalent copper ions in CuAPSO-34 was not significantly affected, whereas, even after a less severe steaming (60 h at 550 °C), these species dramatically decreased in CuZSM-5, and extraframework Al^{3+} ions were simultaneously formed. Consequently, the high activity in N_2O decomposition shown by fresh CuZSM-5 was essentially lost after steaming, while CuAPSO-34 exhibited a significantly milder deactivation.

Keywords: N_2O decomposition; CuZSM-5; CuAPSO-34; Chabasite; Hydrothermal stability; Steam ageing; CO adsorption; FTIR; XRD; BET; Deactivation

1. Introduction

Nitrous oxide (N_2O) is a gas with strong greenhouse effects due to its global warming strength, more than 270 times that of CO_2 [1]. Moreover, N_2O is one of the main contributors to ozone depletion in the stratosphere according to the reaction:

$$N_2O + 3O_3 \rightarrow 2NO_2 + 3O_2. \tag{1}$$

Anthropogenic nitrous oxide is released as a by-product from large-scale chemical processes, such as the production of nitric acid, caprolactam synthesis, the production of adipic acid for the synthesis of Nylon 6-6 and 6-12 [2], and fluidized bed coal combustion [3]. Other nonnegligible sources of nitrous oxide are the internal combustion engines of cars, trucks, etc. [4]. As the lifetime of N_2O is approximately 150 years, in order to reduce its effects on the atmosphere it seems necessary to diminish all kinds of emissions of this gas, as recently cited by the United Nation Framework on Climate Change (Kyoto, Japan, 1997).

The catalytic decomposition of N_2O to N_2 and O_2 is very attractive in principle as it does not require any reducing agent and is strongly favored by thermodynamics. In recent years, many catalysts have been investigated for this reaction, such as noble metals (Rh, Pd) [5,6], transition metal oxides, perovskites [7,8], hydrotalcites [9,10], and zeolites exchanged with noble and transition metal ions [11–14]. Among these, metal-exchanged ZSM-5 zeolites are of growing interest for their low cost and high performances under clean laboratory conditions. Moreover, such catalysts are unique with regard to the properties of copper and the ability to decompose nitric oxide into N_2 and O_2. However, their lack of stability under real operating conditions seems to be an unavoidable limitation [15,16], despite many attempts to stabilize the activity under hydrothermal conditions, using various promoters (La, Ce, Ag) [17–19].

---

[*] Corresponding author.
E-mail address: leonardo.marchese@unito.it (L. Marchese).

0021-9517/03/$ – see front matter © 2003 Elsevier Science (USA). All rights reserved.
doi:10.1016/S0021-9517(03)00033-2

In this context, silicoaluminophosphate molecular sieves with chabasite-related structures, such as SAPO-34, appear attractive because they exhibit a high thermal stability with respect to zeolites. Their thermal resistance was extensively studied via multinuclear NMR [20] and XRD [20–22], which revealed an excellent stability of the framework up to 1000–1200 °C. A tridimitic dense phase appears only at 1000 °C [22], but even at this temperature the zeolitic framework is present in appreciable amounts. Framework stability was also observed for CoAPSO-34 and CuAPSO-34, as recently shown by XRD investigations [23]. In fact, these materials are thermally stable up to 900 °C with the appearance of only a small fraction of the tridimite phase.

The preparation method appears to play a significant role in the hydrothermal stability, the materials prepared via a one-pot procedure being more stable than the corresponding metal-exchanged analogues obtained via conventional postsynthesis ion-exchange treatments. Crystallinity loss is very significant even at 800 °C and complete at 900 °C over copper-exchanged SAPO-34, as recently highlighted by in situ XRD studies [24].

Nevertheless, the interest in such materials has been mainly focused on their applications as catalysts for petrochemical processes (cracking and isomerization, MTO, ODH, etc.), as reported in two recent reviews by Hartmann and Kevan [25] and Stöcker [26]; while studies concerning the use of these new zeo-type materials in NO_x reactions have been limited [27–32].

Ishihara et al. [27,29,30] found a good activity of the Cu-exchanged SAPO-34 system in the NO-SCR with propane in the presence of oxygen. Their XRD ^{27}Al, ^{28}Si, and ^{31}P NMR analyses revealed high hydrothermal resistance—up to 700 °C for 5 h in water stream (15% vol)—of both the framework and the copper phase. Děděcěk et al. [31] obtained promising results in the decomposition of NO over CuMeAPO-11 (Me $= Mg^{2+}$ and Zn^{2+}) and found relevant analogies between the copper features of these materials and those of CuZSM-5 zeolite.

Spectroscopic studies of NO adsorption on CoAPO-18, CoAPO-5 [33], CoAPO-34 [32], and CuSAPO-34 [34,35] highlighted the potential de-NO_x properties of these catalysts. In addition, interesting results in the reduction of NO with CO in the absence of oxygen, decomposition of N_2O, and oxidation of NO with O_2 have been recently shown over copper-alumino and copper-silicoaluminophosphates [36,37], tested in both the presence and the absence of water [24].

In this work, the catalytic activity and hydrothermal stability of CuAPSO-34 catalysts have been studied using the decomposition of N_2O as a probe reaction. The materials were prepared via one-pot synthesis [24,36,37] by directly adding CuO to the synthesis gels. The results obtained have been compared to the catalytic performances of copper-exchanged ZSM-5 zeolite under identical conditions.

The higher hydrothermal stability of CuAPSO-34 and the consequent higher catalytic activity for N_2O decomposition in the presence of water, when compared to CuZSM-5, will be demonstrated.

2. Experimental

2.1. Materials syntheses

The CuAPSO-34 sample was synthesized as follows: After adding CuO to a diluted solution of orthophosphoric acid and stirring at 80 °C until complete dissolution, $Al(OH)_3$ was added at room temperature, with vigorous stirring, until a homogeneous gel was formed. Subsequently, SiO_2 and morpholine were added, again under stirring. The resulting gel with molar composition 0.08 CuO:0.2 SiO_2:0.46 Al_2O_3:0.45 P_2O_5:1.25 morpholine:50 H_2O was crystallized in Teflon-lined autoclaves under autogeneous pressure at 190 °C for 7–10 days. The crystalline product was filtered, washed with water, and dried in air. The CuZSM-5 sample was prepared by ion exchange in aqueous solution starting from a commercial H-ZSM-5 zeolite (Zeolyst CBU-5020) with a Si/Al ratio of 25 and a BET specific area of 400 $m^2\,g^{-1}$. Copper(II) acetate monohydrate (Aldrich purity 99.8%) was used as precursor salt. The parent zeolite was exchanged at 50 °C for 60 min in a solution 20 mM of Cu^{2+} ions. After the ion exchange, the sample was centrifuged, washed in doubly distilled water, and dried at 120 °C overnight. The copper loading in the final products was determined by ICP-AE, which yielded 1.23 wt% for CuAPSO-34 and 1.1 wt% for CuZSM-5.

2.2. Material characterization and catalysis

X-ray diffraction (XRD) patterns were obtained with a Shimadzu XRD 6000, with Cu-K_α radiation. The diffractograms were measured at 200 °C (using a Shimadzu heating accessory Model HA1001) to remove adsorbed water from the calcined samples exposed to air which, in the case of CuAPSO-34, causes an apparent loss of their crystallinity [22,38]. FTIR spectra of adsorbed CO on pelletized samples were recorded at room temperature with a Mattson Research Series Spectrometer in specially designed cells permanently connected to a vacuum line, thereby allowing in situ adsorption–desorption experiments. The as-synthesized CuAPSO-34 was calcined following the procedure reported in Ref. [22]. The final calcination treatment was performed at 550 °C under pure oxygen. Prior to spectroscopic measurements, the samples were outgassed at 550 °C for 4 h (herein named *fresh catalysts*), a treatment which leads to the formation of the catalytically active Cu^+ species [37].

Catalytic activity tests of N_2O decomposition under both dry and wet conditions were carried out with a fixed-bed flow microreactor heated by an electrical oven. The reactor temperature was monitored by a “K”-type thermocouple, placed in a quartz tube, coaxial and internal to the reactor. The gas analysis was carried out with continuous analyzers

(Hartmann & Braunn URAS 10E and MAGNOS 6G) to measure the concentrations of N_2O and O_2. Brooks mass flow controllers (5850S) were used to maintain the flow rates of high-purity gases: N_2O (1% vol) + He (He 99.998%), thus allowing a gas mixture with controlled composition to be fed.

The standard conditions of activity tests were N_2O (600 ppm), and balance He, catalyst mass (W) to gas flow rate (F) ratio $W/F = 0.10\ \mathrm{g\,s\,N\,cm^{-3}}$. Wet gas feeds were obtained by saturating the helium stream at room temperature. The water concentration in the feed was 2.5 vol%. Before each run, CuAPSO-34 was treated at 600 °C under He flow for 2 h, whereas Cu-ZSM-5 was treated at 550 °C in order to obtain the reduced form of copper ions [39–43].

The effect produced by water vapor on the catalytic performances was determined by measuring the activity under dry conditions after the following ageing cycle: (a) ageing under reaction flow, heating the sample from 300 to 550 °C (650 °C for CuAPSO-34) in the presence of water (2.5% vol); (b) ageing in a wet helium flow (H_2O 2.5% in vol) at 550 °C (600 °C for CuAPSO-34) overnight; (c) repeated step (a). The procedure (steps (a) to (c)) was repeated two times. The overall exposure of the catalysts to wet mixtures was 60 h at 550 °C (600 °C for CuAPSO-34). The solids so prepared are herein referred to as *aged catalysts*. A third ageing cycle was run only for CuAPSO-34 (20 h at 600 °C).

3. Results and discussion

3.1. X-ray powder diffraction

The X-ray powder diffraction patterns of the samples were recorded in order to have direct information on the stability of the zeolite structure after the ageing treatment in H_2O. Fig. 1A shows that, after the ageing treatment, Cu-ZSM-5 maintains a good crystallinity without a significant loss in the intensity of the diffraction peaks. This behavior is in good agreement with BET data revealing that the surface area is substantially retained (365 $m^2\,g^{-1}$ of the fresh sample in comparison with 363 $m^2\,g^{-1}$ in the aged sample; Table 1).

Table 1
Specific BET area for fresh and aged CuZSM-5 and CuAPSO-34

Sample	S_{BET} [$m^2\,g^{-1}$]	
	Fresh	Aged
CuZSM-5	365	363
CuAPSO-34	346	198

CuAPSO-34 undergoes a limited crystallinity loss upon hydrothermal treatment, correlated with the presence of reflections of smaller intensity (Fig. 1B). This result agrees with the BET data which revealed an approximately 40% decrease of the surface area upon application of the ageing treatment to the CuAPSO-34 sample (346 $m^2\,g^{-1}$ versus 198 $m^2\,g^{-1}$; Table 1).

3.2. IR spectroscopy of adsorbed CO

CO adsorption is a widely used tool for monitoring the catalyst sites on ion-exchanged zeolites because it gives information about the oxidation state, coordination, and concentration of metal cations. In order to elucidate the nature of catalytic active sites, CO adsorbed on CuAPSO-34 has been compared to that carried out on Cu-ZSM-5 which, under dry conditions, represents one of the most active systems in N_2O decomposition [11] and the most active by far for the decomposition of NO [12].

Fig. 2 shows the infrared spectra of the fresh CuZSM-5 catalyst under decreasing doses of CO adsorbed at room temperature. At higher pressures, the spectra consist of two intense bands at 2177 and 2151 cm^{-1} which decrease progressively with decreasing CO dose, with concomitant formation of a new strong and symmetric band with a maximum at 2157 cm^{-1}. This band is stable under vacuum at room temperature. According to the literature, the bands at 2177 and 2151 cm^{-1} are assigned to the symmetric and

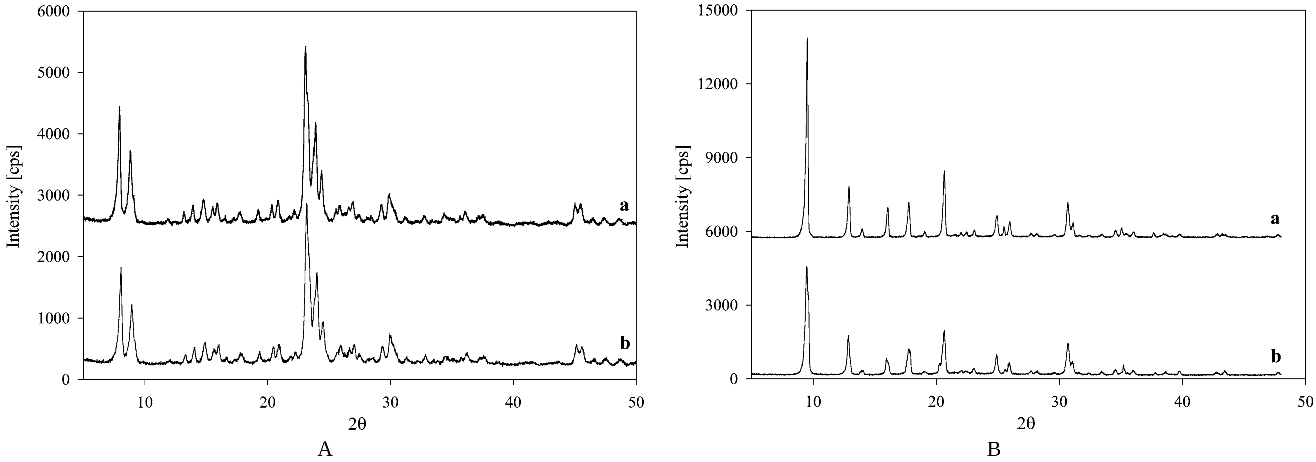

Fig. 1. X-ray powder diffraction recorded at 200 °C of Cu-ZSM-5 (A) and CuAPSO-34 (B): (a) fresh samples; (b) after hydrothermal ageing treatment.

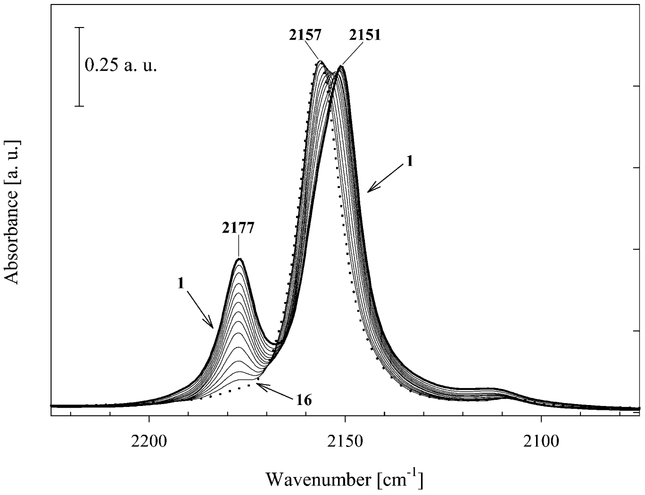

Fig. 2. FTIR spectra of CO adsorbed at room temperature at decreasing equilibrium pressures on fresh Cu-ZSM-5 catalyst. Curve 1, $p_{CO} = 30$ Torr; curve 16, under vacuum.

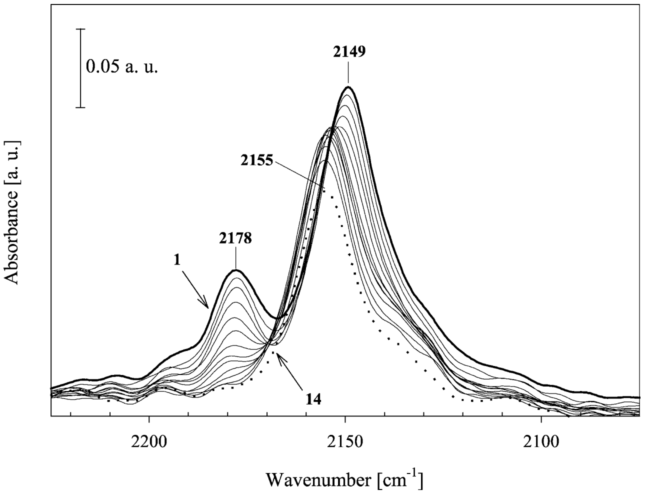

Fig. 3. FTIR spectra of CO adsorbed at room temperature at decreasing equilibrium pressures on fresh CuAPSO-34 catalyst. Curve 1, $p_{CO} = 30$ Torr; curve 14, under vacuum.

asymmetric stretching vibrations of Cu(I)$(CO)_2$ dicarbonyl species; and the band at 2157 cm^{-1} to the CO stretching of Cu(I)CO monocarbonyl complexes [44–46].

CO adsorbed on fresh CuAPSO-34 (Fig. 3) leads to the formation of bands at 2149, 2178, and 2155 cm^{-1} which show a pressure dependence very similar to that reported for Cu-ZSM-5: they are consequently assigned to dicarbonyl and monocarbonyl complexes formed on Cu(I) sites in the chabazite structure. This result strongly suggests that extraframework Cu^+ ions are present in CuAPSO-34 after the activation treatment [23,37]. Moreover a shoulder at 2150–2125 cm^{-1} of the carbonyls band indicates the presence of copper oxidic aggregates in CuAPSO-34 catalysts.

However, the bands of dicarbonyls and monocarbonyls formed on the CuAPSO-34 catalyst are less intense (around 5 times) and broader than in Cu-ZSM-5. This result indicates that in CuAPSO-34 there is a lower concentration of accessible Cu^+ centers, which are located in a wider variety of sites. Three different cationic sites in dehydrated ion-exchanged synthetic and natural chabasite have been found by a photoluminescence study by Děděcěk et al. [47]. As far as zeolites with a low aluminum content are concerned, Nachtigallova et al. [48] suggested that two type of sites are present in Cu-ZSM-5: Cu(I) ions located at the channel intersection in more open coordination, and Cu(I) ions coordinated to the six-membered ring in a more packed environment. Lamberti et al. [44] also reported that two families of Cu(I) sites, which are characterized by different coordinative unsaturation, are present in CuZSM-5.

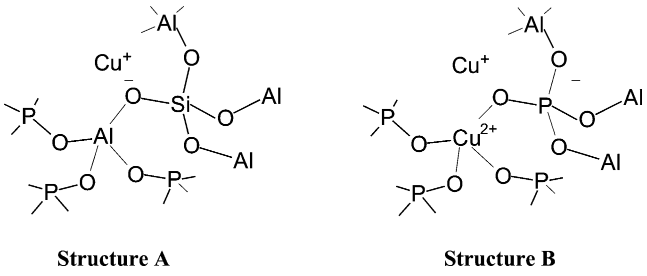

Scheme 1.

Moreover, the fact that the distribution of Cu(I) in CuAPSO-34 is more heterogeneous than in Cu-ZSM-5 can be also explained by considering that exchangeable sites of CuAPSO-34 may be produced either by substitution of phosphorous with silicon (Scheme 1, structure A) or by isomorphous substitution of aluminum ions with cupric ions in tetrahedral sites (Scheme 1, structure B). In particular, the presence Cu^{2+} framework sites is typical of Cu-aluminophosphates prepared by adding copper salt directly to the synthesis gel [36,37]. The fact that the bands assigned to dicarbonyl and monocarbonyl complexes formed on Cu(I) sites in CuAPSO-34 are less intense than Cu-ZSM-5, prepared via an ion-exchange procedure with similar Cu loading, is an indication that part of the copper ions are inserted in the aluminophosphate framework.

The comparison of the spectra of CO adsorbed at room temperature on fresh and aged Cu-ZSM-5 and CuAPSO-34 catalysts is reported in Figs. 4 and 5, respectively.

CO adsorbed on the aged Cu-ZSM-5 sample (Fig. 4, bottom curves) leads to the formation of bands at similar frequencies as found on the fresh catalyst. A new band, however, is found at about 2190 cm^{-1} in the case of the aged sample. It is relevant to point out that the concentration of dicarbonyl and monocarbonyl complexes is drastically reduced as a consequence of the hydrothermal treatment. The absorption at 2190 cm^{-1} is assigned to CO coordinated to extraframework aluminum ions [46].

The comparison between fresh and aged CuAPSO-34 catalysts (Fig. 5) shows that the intensity of the bands of the carbonyls is not significantly affected by the hydrothermal treatment. However, a slight broadening of the band at 2155 cm^{-1} and an increase of the shoulder at 2150–

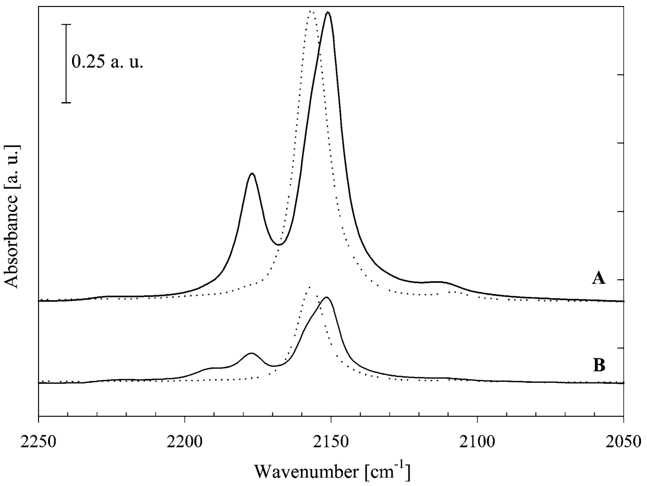

Fig. 4. Comparison of FTIR spectra of CO adsorbed at room temperature between (A) fresh Cu-ZSM-5 and (B) aged Cu-ZSM-5. Solid lines, $p_{CO} = 30$ Torr; dotted lines, under vacuum.

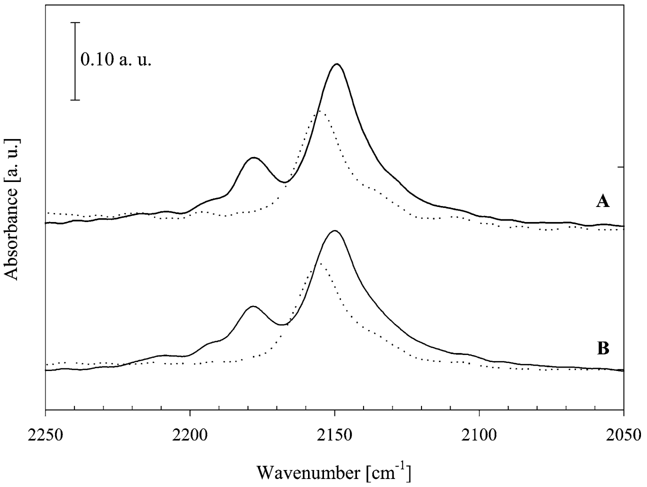

Fig. 5. Comparison of FTIR spectra of CO adsorbed at room temperature between (A) fresh CuAPSO-34 and (B) aged CuAPSO-34. Solid lines, $p_{CO} = 30$ Torr; dotted lines, under vacuum.

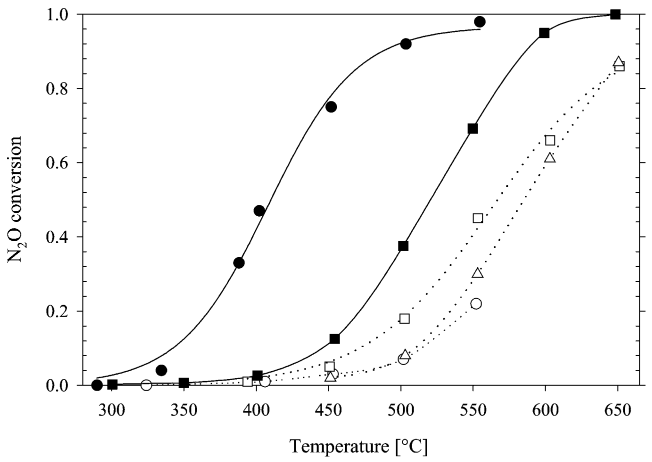

Fig. 6. N_2O conversion as a function of temperature over Cu-ZSM-5 (●) and CuAPSO-34 (■). Feed: N_2O (600 ppm), H_2O (2.5% vol only for CuAPSO-34, △), and balance He. $W/F = 0.10$ g s N cm^{-3}. Open symbols represent the activity data obtained after the second ageing cycle.

2125 cm^{-1} indicate that oxidic aggregates are more abundant after steam ageing.

3.3. N_2O decomposition results

Fig. 6 shows the conversion of N_2O as a function of temperature of both fresh and aged CuZSM-5 and CuAPSO-34 catalysts. The data clearly prove that despite the similar metal loading (1.10 and 1.23%, respectively, for CuZSM-5 and CuAPSO-34), fresh CuAPSO-34 is less active than fresh Cu-exchanged ZSM-5, reaching complete conversion at 650 °C instead of 550 °C. The activity of CuAPSO-34 is about one order of magnitude lower than CuZSM-5, in agreement with the intensity of the bands of adsorbed CO (compare Figs. 2 and 3).

However, the catalytic performances of CuAPSO-34 catalyst appeared much less affected by hydrothermal ageing than that of CuZSM-5. As a matter of fact, while fresh CuZSM-5 reached 98% conversion at 550 °C, after the second ageing cycle its conversion reaches only 20%. On the contrary, CuAPSO-34 achieves 45% of conversion at the same temperature.

These data revealed that the active sites, e.g., the Cu^+ ions, are more stabilized by the chabasite framework of SAPO-34, an observation also clearly revealed by IR experiments of adsorbed CO on aged and fresh catalysts (compare the results of Figs. 4 and 5). Thus, the activity loss due to the hydrothermal ageing should be related to the partial loss of the CuAPSO-34 chabasite structure (as found by XRD and BET measurements) rather than to the modification of the environment of the copper ions. It can be, therefore, proposed that copper ions in the chabasite structure are more strongly bound to the zeolitic framework than in ZSM-5, and this effect might be related to the presence of structural Cu^{2+} ions (Scheme 1).

However, steam ageing treatments do not affect the Cu-ZSM-5 structure, in agreement with previous results [49–52], but strongly modify the environment of the copper ions. Due to the dealumination of the CuZSM-5 zeolite, revealed by the presence of Al^{+3} extraframework species, copper ions are forced to migrate to inactive positions probably segregating in oxidic clusters [19,50].

The higher hydrothermal stability of CuAPSO-34 results in its ability to carry out the reaction even in the presence of water in concentrations similar to those found in industrial applications [5], as reported in Fig. 6. The activity of CuAPSO-34, in fact, suffers only a slight inhibition in the presence of water, most likely due to the competition between N_2O and water molecules for copper sites especially at lower temperature. This result is even more important considering that, under the same experimental conditions, CuZSM-5 did not show any appreciable or steady-state activity in wet mixtures.

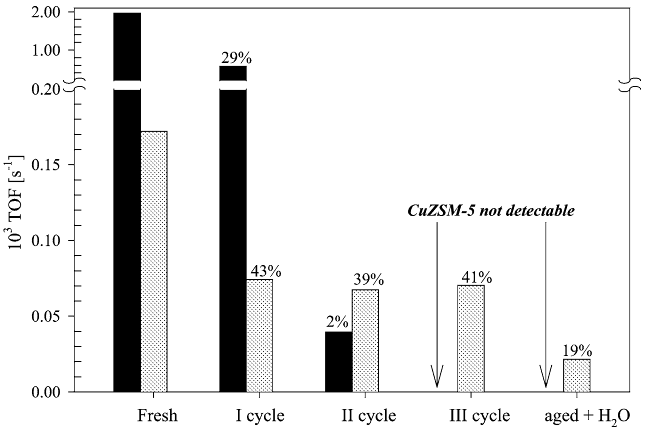

Fig. 7. Hydrothermal deactivation of Cu-ZSM-5 (black) and CuAPSO-34 (gray) expressed in terms of turnover frequency (TOF) in N_2O decomposition at 450 °C. Feed: N_2O (600 ppm), H_2O (2.5% in vol when fed), and He (balance). $W/F = 0.10\ \mathrm{g\,s\,N\,cm^{-3}}$.

The high hydrothermal stability of CuAPSO-34 is further highlighted in Fig. 7 where the catalytic performances obtained after each ageing cycle are reported. It is clear that the continuous exposition to water streams results in the progressive and irreversible deactivation of CuZSM-5, which did not show any appreciable activity after the third ageing cycle under neither dry nor wet conditions. On the contrary, CuAPSO-34 reaches a stable condition already after the first ageing cycle and its activity remains unaffected by further cycles, the aged sample showing significant performances even in the presence of water (about 19% of fresh activity, which was measured in the absence of water).

4. Conclusions

The hydrothermal stability of copper silicoaluminophosphates with chabasite-like structures has been extensively investigated in the catalytic decomposition of nitrous oxide, and compared with CuZSM-5. Measurements of the porosity properties proved that prolonged expositions to wet streams at high temperature do not significantly affect the MFI framework of CuZSM-5, whereas CuAPSO-34 showed slight modifications of both crystallinity and BET specific area.

FTIR investigation of adsorbed CO revealed the presence of copper extraframework species (i.e., Cu^+ ions) in the CuAPSO-34 sample, which exhibit similar properties to copper-exchanged ions in CuZSM-5. However, upon steaming, the concentration of monovalent copper ions in CuAPSO-34 was not significantly affected, whereas even after a less severe steaming (60 h at 550 °C), these species decreased dramatically in CuZSM-5. The dealumination of CuZSM-5 catalysts upon steaming (revealed by the presence of extraframework Al^{3+} species) probably causes the loss of copper active species. Consequently, the higher initial activity in N_2O decomposition showed by CuZSM-5 was nearly completely suppressed by steam ageing while CuAPSO-34 exhibited a limited deactivation, keeping a measurable activity even in the presence of water.

Acknowledgments

Funding by the Italian MURST (Progetti di Rilevante Interesse Nazionale, Cofinanziamento 2000) and Brazilian FAPESP (Fundação e Amparo à Pesquisa no Estado de São Paulo) are acknowledged. The precious assistance of Mrs. Assunta Viola for the catalytic tests are highly appreciated. M. Cadoni acknowledges ASP (Associazione per lo Sviluppo Scientifico e Tecnologico del Piemonte) for financial support.

References

[1] G. Centi, A. Galli, B. Montanari, S. Perathoner, A. Vaccari, Catal. Today 35 (1997) 113.
[2] J. Werther, T. Ogada, C. Philippek, in: Proc. of 6th Internat. Workshop on Nitrous oxide Emission, Turku, Finland, 1995, p. 139.
[3] B.W. Riley, J.R. Richmond, Catal. Today 17 (1993) 277.
[4] M. Berges, R. Hoffmann, D. Scharffe, P. Crutzen, J. Geophys. Res. 98 (1993) 18527.
[5] K. Yuzaki, T. Yarimizu, K. Aoyagi, S. Ito, K. Kunimori, Catal. Today 45 (1998) 129.
[6] O. Yuichi, K. Kazushi, B. Ming, M. Tatsuo, J. Chem. Phys. B 110 (1999) 8221.
[7] S. Subramanian, C.S. Swamy, Catal. Lett. 35 (1995) 361.
[8] L.Z. Gao, C.T. Au, Appl. Catal. B 30 (2001) 35.
[9] S. Kannan, C.S. Swamy, Appl. Catal. B 3 (1994) 109.
[10] J.N. Armor, T.A. Braymer, T.S. Farris, Y. Li, F. Petrocelli, E.L. Weist, S. Kannan, C.S. Swamy, Appl. Catal. B 7 (1996) 397.
[11] F. Kapteijn, J. Rodriguez-Mirasol, J.A. Moulijn, Appl. Catal. B 9 (1996) 25.
[12] V.I. Pârvulescu, P. Grange, B. Delmon, Catal. Today 46 (1998) 233.
[13] A. Dandekar, M.A. Vannice, Appl. Catal. B 22 (1999) 179.
[14] Z. Schay, L. Guczi, A. Beck , I. Nagy, V. Samuel, S.P. Mirajkar, A.V. Ramaswamy, G. Pál-Borbély, Catal. Today 75 (2002) 393.
[15] J.N. Armor, Micropor. Mesopor. Mater. 22 (1998) 451.
[16] Y. Traa, B. Burger, J. Weitkamp, Micropor. Mesopor. Mater. 30 (1999) 3.
[17] A.V. Kucherov, C.P. Hubbard, T.N. Kucherova, M. Shelef, Kinet. Catal. 38 (1997) 607.
[18] Z. Chajar, P. Denton, F. Berthet de Bernard, M. Primet, H. Praliaud, Catal. Lett. 55 (1998) 217.
[19] Y. Zhang, M. Flytzani-Stephanopoulos, J. Catal. 164 (1996) 131.
[20] Y. Watanabe, A. Koiwai, H. Takeuchi, Shi-Aki Hyodo, S. Noda, J. Catal. 143 (1993) 430.
[21] S.T. Wilson, B.M. Lok, C.A. Messina, T.R. Cannan, E.M. Flanigen, J. Am. Chem. Soc. 104 (1982) 1146.
[22] L. Marchese, A. Frache, G. Gatti, S. Coluccia, L. Lisi, G. Ruoppolo, G. Russo, H.O. Pastore, J. Catal. 208 (2002) 479.
[23] A. Frache, B. Palella, M. Cadoni, R. Pirone, P. Ciambelli, H.O. Pastore, L. Marchese, Catal. Today 75 (2002) 359.
[24] A. Frache, B. Palella, M. Cadoni, R. Pirone, H.O. Pastore, L. Marchese, Top. Catal. (2002) 53.
[25] M. Hartmann, L. Kevan, Chem. Rev. 99 (1999) 635.
[26] M. Stöcker, Micropor. Mesopor. Mater. 29 (1999) 3.
[27] T. Ishihara, M. Kagawa, Y. Mizuhara, Y. Takita, Chem. Lett. (1992) 2119.
[28] D. Panayotov, L. Dimitrov, M. Khristova, L. Petrov, D. Mehandjiev, Appl. Catal. B 6 (1995) 61.

[29] T. Ishihara, M. Kagawa, F. Hadama, Y. Takita, J. Catal. 169 (1997) 93.
[30] T. Ishihara, M. Kagawa, F. Hadama, H. Nishiguchi, M. Ito, Y. Takita, Ind. Eng. Chem. Res. 36 (1997) 17.
[31] J. Děděcěk, J. Čejka, B. Wichterlova, Appl. Catal. B 15 (1998) 233.
[32] L. Marchese, E. Gianotti, B. Palella, R. Pirone, G. Martra, S. Coluccia, P. Ciambelli, Stud. Surf. Sci. Catal. 130C (2000) 3005.
[33] E. Gianotti, L. Marchese, G. Martra, S. Coluccia, Catal. Today 54 (1999) 547.
[34] D.B. Akolekar, S.K. Bhargava, K. Foger, J. Chem. Soc., Faraday Trans. 94 (1999) 155.
[35] D.B. Akolekar, S.K. Bhargava, J. Mol. Catal. A 157 (2000) 199.
[36] A. Frache, M. Cadoni, S. Coluccia, L. Marchese, B. Palella, R. Pirone, P. Ciambelli, Stud. Surf. Sci. Catal. 135 (2001) 328.
[37] A. Frache, L. Marchese, M. Cadoni, S. Coluccia, B. Palella, R. Pirone, P. Ciambelli, Stud. Surf. Sci. Catal. 140 (2001) 269.
[38] M. Briend, R. Vomscheid, M.J. Peltre, P.P. Man, D. Barthomeuf, J. Phys. Chem. 99 (1995) 8270.
[39] M. Iwamoto, H. Hamada, Catal. Today 10 (1991) 57.
[40] A.W. Aylor, S.C. Larsen, J.A. Reimer, A.T. Bell, J. Catal. 157 (1995) 592.
[41] G. Spoto, A. Zecchina, S. Bordiga, G. Ricchiardi, G. Martra, G. Leofanti, G. Petrini, Appl. Catal. B 3 (1994) 151.
[42] B.L. Trout, A.K. Chakraborty, A.T. Bell, J. Phys. Chem. B 100 (1996) 17582.
[43] A.T. Bell, Catal. Today 38 (1997) 151.
[44] C. Lamberti, S. Bordiga, M. Salvalaggio, G. Spoto, A. Zecchina, J. Phys. Chem. B 101-3 (1997) 344.
[45] A. Zecchina, S. Bordiga, M. Salvalaggio, G. Spoto, D. Scarano, C. Lamberti, J. Catal. 173 (1998) 540.
[46] J. Datka, B. Gil, M. Kawalek, B. Staudte, J. Mol. Struct. 511 (1999) 133.
[47] J. Děděcěk, B. Wichterlova, P. Kubat, Micropor. Mesopor. Mater. 32 (1999) 63.
[48] D. Nachtigallova, P. Nachtigall, J. Sauer, Phys. Chem. Chem. Phys. 3 (2001) 1552.
[49] A.V. Kucherov, C.P. Hubbard, M. Shelef, J. Catal. 157 (1995) 603.
[50] K.C.C. Kharas, H.J. Robota, D.J. Liu, Appl. Catal. B 2 (1993) 225.
[51] M. Iwamoto, J. Wang, K.M. Sperati, T. Sajiki, M. Misono, Chem. Lett. (1997) 1281.
[52] J.Y. Yan, G.D. Lei, W.M. Sachtler, H.H. Kung, J. Catal. 161 (1996) 43.